University of Birjand

Water Harvesting Research (2025) Vol. 8, No. 2: 207-227

10.22077/jwhr.2025.9858.1184

ORIGINAL ARTICLE

Groundwater Depletion in an Arid Aquifer: Insights from Long-Term MODFLOW Modeling of the Kerman Plain

Bahareh Mirkamandar[a], Mohammad Bagher Rahnama[b], Mohammad Zounemat-Kermani[c*]

[a]Ph.D Candidate, Department of Water Engineering, Faculty of Agriculture, Shahid Bahonar University of Kerman, Kerman, Iran.
[b]Associate Professor, Department of Water Engineering, Faculty of Agriculture, Shahid Bahonar University of Kerman, Kerman, Iran.
[c]Professor, Department of Civil Engineering, Shahid Bahonar University of Kerman, Kerman, Iran.

[*]Corresponding Author E-mail address: zounemat@uk.ac.ir
Received: 01 August 2025, **Revised**: 16 September 2025, **Accepted**: 20 September 2025

Abstract

The significant impact of climate change, reduced precipitation, and drought in recent decades has led to a marked decline in both surface and groundwater levels. This crisis has particularly affected regions with arid and semi-arid climates, resulting in excessive abstraction from various aquifers. The Kerman Plain aquifer, which is located in an arid to semi-arid region, has also experienced a severe drop in groundwater levels over these years. Therefore, quantitative assessment of groundwater levels in this plain is of great importance for improving management and decision-making during serious water crises. In the present study, a 22-year simulation of groundwater levels in the plain was conducted using the GMS software and the MODFLOW numerical model. Future aquifer conditions up to the point of reaching the bedrock were predicted based on groundwater levels in the Bodaghabad well, located in the northern part of the aquifer within the Kerman urban area. According to the modeling results for the period 2002–2024, the greatest annual decline was observed in the western and eastern regions, averaging 1.23 meters, while the minimum decline 0.27 meters per year occurred in the central and southern parts of the aquifer. Furthermore, the findings showed that the diversion of Kerman's urban wastewater for use by adjacent industries, and the consequent lack of aquifer recharge from the city's natural wastewater drainage, have increased the groundwater level decline rate by 15.85% and shortened the time to reach bedrock in the Kerman urban area by 14 years.
Keywords: GMS-MODFLOW, Groundwater, Kerman aquifer, Modeling, Natural recharge

1. Introduction

Nowadays, the excessive exploitation of groundwater reservoirs for various purposes including agriculture, drinking water, and industry is driven by factors such as climate change and the resulting droughts, population growth, industrial and agricultural development, and increasing urbanization and cultural shifts. Moreover, the mismanagement of groundwater extraction leads to land subsidence, seawater intrusion into freshwater resources, and the deterioration of both the quantity and quality of these vital reserves. In an aquifer experiencing depletion and excessive withdrawal, management strategies must be implemented to prevent such adverse effects both at present and in the future.

The Kerman Plain aquifer has not been immune to these detrimental impacts; excessive groundwater extraction through both licensed and unlicensed wells in this arid and semi-arid region has resulted in a severe decline in water levels and has precipitated a critical condition in the groundwater reserves. These challenges highlight the necessity of comprehensive investigations through various modeling approaches and the formulation of appropriate policies to improve the condition of the regional aquifer.

Quantitative assessment of groundwater resources is inherently complex and, in practice, requires considerable time and financial investment. Therefore, the application of numerical models and related simulations can serve as an effective tool for examining and analyzing these vital resources.

Groundwater level fluctuations in the Zanjan Plain were simulated using the finite difference numerical method. The model was run, assuming a declining rate of groundwater and a constant recharge over a 15-year period from 2007 to 2022. The resulting groundwater level maps for these years indicated a severe decline in water table levels due to continued over-extraction of groundwater from the Zanjan aquifer (Panahi et al., 2017).

Groundwater flow paths in the Hamadan-Bahar Plain aquifer were simulated using GMS software, based on geological, hydraulic, and hydrological data. In this study, a three-dimensional hydrological model of the Hamadan-Bahar Plain was first developed, and then groundwater flow in the plain was simulated using the numerical MODFLOW code. Additionally, estimation of groundwater flow paths was carried out using the MODPATH code.

The results of the flow path simulation indicated that groundwater moves from the aquifer boundaries towards the center and the discharge zones, following the hydraulic gradient. Overall, continuation of the current groundwater flow regime will increase contamination levels in the aquifer and may cause irreversible damage to the groundwater reservoir (Bayat et al., 2018). Using the numerical code MT3DMS, the transport of solutes, particularly the movement of salinity and the concentration of dissolved salts in the Malekan

Plain aquifer, was simulated. The results indicated that this model, in addition to its good capability in describing the actual behavior of the system, demonstrated that excessive groundwater abstraction has led to a decline in the groundwater table and accelerated the intrusion of saline water into the northwestern part of the plain, resulting in both quantitative and qualitative deterioration of the aquifer in this section (Azizi et al., 2019).

The Toyserkan Plain Aquifer, located in Hamadan Province, was modeled using the MODFLOW numerical code under two ten-year scenarios. The first scenario involved the continuation of the current extraction trend, while the second scenario was defined as a 20% increase in irrigation efficiency in the study area, accompanied by reduced groundwater withdrawals. The results indicate that, under both scenarios, a decline in the groundwater table across the plain is evident (Taheri and Kamali, 2019).

A study aimed at delineating the mixing zone for the TDS parameter and assessing variations in river TDS concentration, using the MODFLOW and MT3D models, investigated the behavior of the aquifer adjacent to the Zarjoub River during both agricultural and non-agricultural seasons. The results indicated that in the non-agricultural season, the mixing zone is located at a distance of 20 meters from the river, whereas in the agricultural season, this distance decreases significantly to less than 20 meters. Subsequently, to delineate the mixing zone for the NO_3 parameter, the MODFLOW and RT3D models were employed.

In this stage, the model was run under two scenarios to evaluate the effects of microbial activity. The findings revealed that, in the absence of biodegradation within the mixing zone, the zone lies at a distance of 25 meters from the river; however, when biodegradation is accounted for, the mixing zone shifts to a distance of less than 20 meters (Yousefi et al., 2020). In a study, based on the calculation of the natural groundwater level decline gradient, the effects of recharge and the absence of recharge from wastewater on the rate of groundwater decline in the Kerman Plain and the Nozari well were analyzed and predicted.

The results indicated that the lack of natural wastewater drainage through existing absorption wells in the area, combined with the implementation of the Kerman urban sewerage network and the transfer of wastewater outside the region, would increase the groundwater level decline gradient by 11 % per month. It was also projected that the time required for the groundwater level to reach the bedrock and for the early drying of the region's wells would be approximately 12 years (Mirkamandar et al., 2025).

In another study, the effects of constructing a complete municipal wastewater collection network and fully implementing the treatment plant phase on the quantity and quality of groundwater resources in Ardakan were examined using the MODFLOW numerical model. The modeling results showed that the use of treated effluents to improve and compensate for the drop in water levels in groundwater resources in the Yazd-Ardakan plain can be very effective and prevent at least 23% reduction in groundwater levels (Kamali et al., 2021).

The Effects of various climate change scenarios on groundwater fluctuations in the Kerman Plain were investigated. In this study, GMS software was used to quantitatively model the groundwater in the plain under steady-state conditions for October of the 2002–2003 water year, under unsteady-state conditions over the period 2002–2012 in 120-time steps, and for model validation during the 2012–2015 period. According to the reported results, under various scenarios, the groundwater level in the entire region is projected to decline by 7.19, 7.26, and 7.33 meters, respectively, during the future period (2016–2030) compared to the baseline level in 2002–2003.

It was also recommended that authorities take measures to address the overexploitation of groundwater resources by modifying cropping patterns and adopting modern irrigation methods (Jafari et al., 2021). The MODFLOW code in GMS software was used to simulate the groundwater of the Mahabad aquifer for a two-year period from 2010 to 2012. Their model was run in both steady-state and unsteady-state conditions. Its performance was evaluated based on root mean square error (RMSE), mean absolute error (MAE), and coefficient of determination (R^2) for the unsteady state, which were 0.88 m, 0.72 m, and 0.99, respectively. Their study results showed that the Mahabad aquifer is not in a favorable condition and, with increased extraction and reduced precipitation, especially in recent years, its situation will worsen (Sheikha BagemGhaleh et al., 2022).

The MODFLOW model was used to model groundwater in the region, and it was calibrated for the base period (from October 2010 to September 2014). The correlation coefficient of 0.98 in the unsteady state demonstrated the high accuracy of the aquifer's quantitative modeling. Their results showed that groundwater levels in the future period will be higher than in the base period, which can support the development of agriculture and industry in the region (Najafi et al., 2022). The quantitative status of groundwater in the Southern Mahyar–Aseman Plain aquifer was investigated and modeled using fifteen years of data up to 2011, employing the MODFLOW 2005 numerical model in GMS software.

According to final results from the FlowBudget engine during their 125-month modeling period, the average decline in the groundwater table was reported to be 7.5 meters, with the greatest decline occurring in the eastern part of the aquifer (Hoseinzadeh and Ardestani, 2024). The Shamil aquifer in Hormozgan Province was also modeled using the MODFLOW model and groundwater modeling software. Their results showed that the northern, central, and southern parts of the aquifer possess the highest hydraulic conductivity (ranging from 20 to 50 meters per day). According to their projections, if the current trend continues, the groundwater table will decline by 0.4 meters per year over the next ten years (Sabahnia and Sadeghi, 2024).

Given the crucial role of groundwater in meeting various human water demands particularly in arid and semi-arid regions where such reserves are limited quantitative monitoring of aquifers through groundwater level modeling has become increasingly significant. This approach enables optimal management, the development of appropriate management strategies, and effective planning for the sustainable use of these valuable resources.

In recent years, the Kerman Plain aquifer, with an arid and semi-arid climate, has been among those facing critical conditions due to excessive groundwater extraction and the cessation of recharge from wastewater infiltration. From the past until 2018, this aquifer was recharged through absorption wells utilizing municipal wastewater. The natural drainage of wastewater via these wells was considered an effective and practical solution to counteract the depletion of groundwater reserves and land subsidence.

Unfortunately, since 2018, the implementation of the urban sewerage collection system and the transfer of wastewater for industrial uses have altered the groundwater flow dynamics in Kerman City, leading to an abrupt decline in groundwater levels in the area. Therefore, modeling the groundwater table of the aquifer and forecasting its future status, based on the conducted studies, can serve as an effective approach for gaining a deeper understanding of the existing critical conditions, proposing appropriate solutions, and making informed and necessary management decisions.

Given the importance of groundwater resources in the Kerman Plain aquifer for agriculture, potable water supply, and industry and the significant decline in groundwater levels over recent decades precise groundwater modeling is essential for assessing changes in this valuable resource and predicting its future status. The MODFLOW groundwater flow simulation model provides a simplified representation of actual groundwater systems and has been widely employed in general groundwater flow studies (Bejranonda et al., 2009; Dafny et al., 2010; Koch et al., 2012; Lyazidi et al., 2020).

In this study, the groundwater level of the Kerman Plain was modeled and forecasted using the numerical MODFLOW code within the GMS 10.8.8 software, with the aim of proposing practical solutions to enhance groundwater reserves. Furthermore, the impact of implementing the urban sewerage system on the groundwater flow dynamics of Kerman City was evaluated by defining a scenario involving increased recharge from wastewater. The changes in the modeled and predicted groundwater levels resulting from the defined scenarios are illustrated for the Bedagh-Abad well, located in the northern part of the aquifer. These results are comparable to, and can be further interpreted alongside, the findings reported by Mirkamandar et al. (2025) and Kamali et al. (2021), as well as those from other studies addressing a similar research topic.

Moreover, a comparison between the impact of using wastewater for artificial aquifer recharge and the volume of water transferred for industrial purposes demonstrates the extent to which these actions influence groundwater level variations. Such a comparison enables more accurate planning for groundwater allocation across different sectors and supports decision-making aimed at ensuring the sustainability of these resources. The findings of this research provide a deeper understanding of the interactions between groundwater exploitation and industrial water demands and offer valuable insights for sustainable groundwater management in semi-arid environments. It is noteworthy that most previous studies have focused on other plains or regions outside the country, and no research has yet been conducted to quantitatively assess the aquifer in this area by defining scenarios of recharge from wastewater and the absence of such recharge. Therefore, given the importance of the region's water resources, undertaking such modeling is deemed essential.

2. Materials and Methods

2.1. Study Area

The study area of the Kerman plain is located within the geographical coordinates of 56°42′ to 57°20′ eastern longitude and 56°55′ to 57°01′ northern latitude, situated between two mountain ranges that pass through its northeast and southwest. The study area, known as Kerman-Baghain plain, is located within the Kavir Deranjir drainage basin, covering an area of 1,612.15 square kilometers. The urban area of Kerman is located in the east and northeast of the Kerman plain aquifer, covering an area of 154 square kilometers.

The maximum elevation of this plain is 2,100 meters in the southeastern regions, while the minimum elevation is 1,650 meters in the northwestern regions, with an average elevation of 1,830 meters above sea level. The plain is surrounded and enclosed by the Jopar mountains to the south, the Darmano and Tiz mountains to the north, the Bid and Badamo mountains to the west, and the Namvar and Nasr mountains to the east. This area includes one synoptic station located at Kerman Airport, seven automatic rain gauge stations affiliated with the Meteorological Organization, and one standard rain gauge station operated by the Regional Water Company of Kerman Province. Precipitation is one of the most influential parameters affecting the amount of groundwater resources. The long-term average annual precipitation in the Kerman plain has been estimated at 128 millimeters.

Additionally, over the past fifty years, the average maximum temperature recorded at the Kerman synoptic station has been 42°C, the average minimum temperature has been -30°C, and the average annual temperature in this region has been reported to range from 15 to 20°C. Overall, this region has a cold and dry climate. Its winters are cold to very cold, while summers are moderate, semi-warm, and dry (Meteorological Yearbook, 2019). The main and permanent river flowing within the study area is the Chari River, which flows from the southwest of the aquifer toward the west and drains into the Baghain Plain. The geographical location of the studied aquifer, situated in Kerman Province within the boundaries of Kerman city, together with the Bedagh-Abad well selected for this investigation, is shown in Figure 1.

The Bedagh-Abad well, located near the city of Kerman, represents the optimal option for evaluating the various scenarios examined in this study. The data obtained from this well record conditions not captured by other observation wells in the region. Moreover, its measurement records are reliable in terms of temporal coverage, continuity, and data quality, enabling their effective use for model calibration and validation. Overall, the observed pumping characteristics and groundwater level fluctuations in this well are consistent with the prevailing conditions of the study area, ensuring its suitability as a representative indicator of aquifer behavior in the Kerman region.

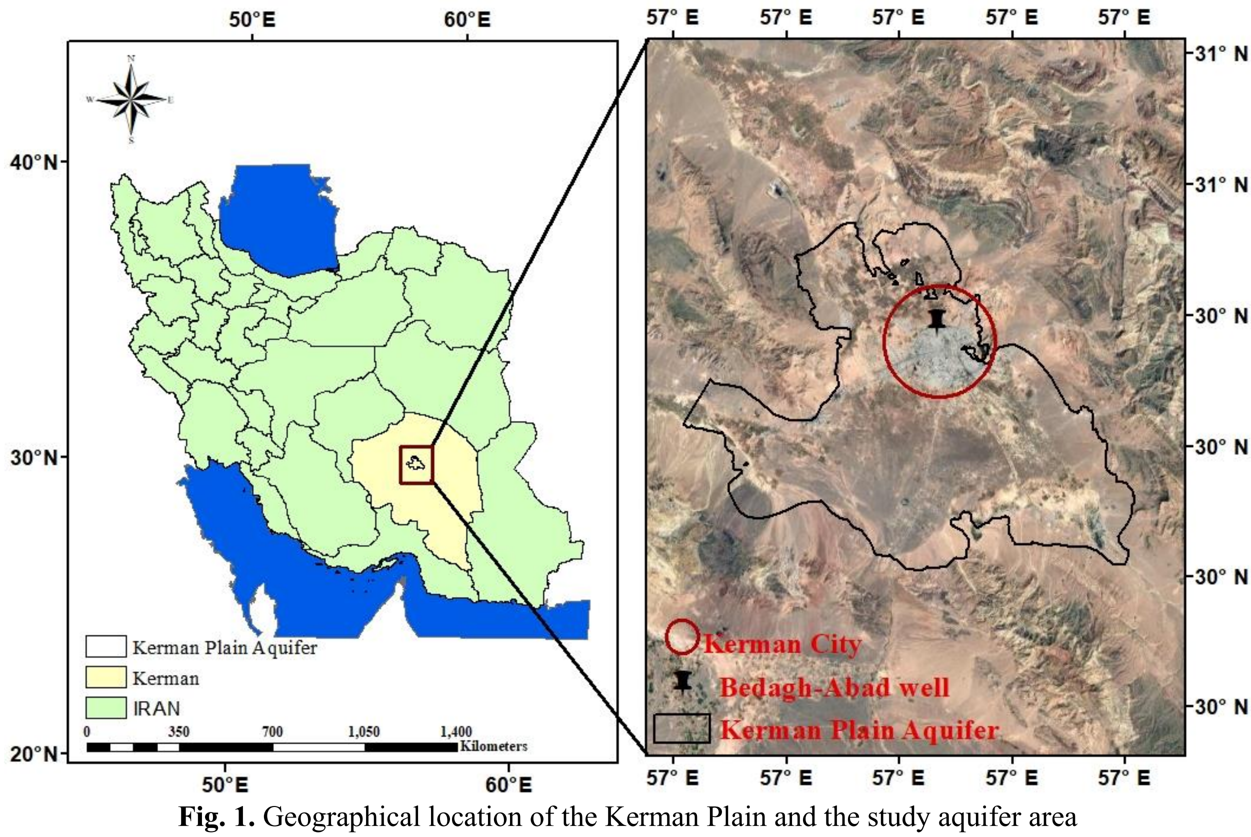

Fig. 1. Geographical location of the Kerman Plain and the study aquifer area

2.2. Introduction to GMS groundwater modeling software

A groundwater model is a tool for conceptualizing and graphically representing the behavior of subsurface physical systems using mathematical equations. Through such models, the factors influencing groundwater resources and the changes in their storage volume can be precisely monitored and controlled, allowing for future projection of aquifer conditions to support sustainable groundwater management and use (Anderson and Woessner, 1995).

The Groundwater Modeling System (GMS) is a comprehensive graphical environment for groundwater simulation, developed by the United States Army Corps of Engineers

Research Laboratory. This modeling platform supports various types of numerical models and enables data exchange between different models, as well as data import from a wide range of formats and external software.

GMS offers numerous tools for describing the study area, developing conceptual models, generating meshes and grids, and performing pre- and post-processing of simulation results. Utilizing finite difference and finite element methods, GMS is capable of both quantitative and qualitative groundwater modeling. The software encompasses dozens of mathematical codes for different simulation purposes; all integrated in a modular architecture. The governing equation for groundwater flow in a porous medium is obtained by combining the continuity equation with Darcy's law, with its general form expressed as follows:

$$\frac{\partial}{\partial x}\left(-k_x\frac{\partial h}{\partial x}\right)+\frac{\partial}{\partial y}\left(-k_y\frac{\partial h}{\partial y}\right)+\frac{\partial}{\partial z}\left(-k_z\frac{\partial h}{\partial z}\right) = S_s\frac{\partial h}{\partial t} \pm q_s \quad (1)$$

h: Hydraulic head (m), t: Time (s), k: Hydraulic conductivity $(\frac{m}{s})$, q_s: Source or sink term per unit volume of aquifer $\left(\frac{m^3}{s}\right)$, S_s: Specific storage coefficient $\left(\frac{1}{m}\right)$.

If the flow domain is assumed to be homogeneous and isotropic (k is independent of x, y, and z), the above equation simplifies to Equation (2). if the groundwater flow is steady-state and there is no source or sink (e.g., no spring or well) between the two selected sections, the groundwater flow equation simplifies to the Laplace equation, as expressed in Equation (3).

$$\frac{\partial^2 h}{\partial x^2}+\frac{\partial^2 h}{\partial y^2}+\frac{\partial^2 h}{\partial z^2}=\frac{S_s}{K}\frac{\partial h}{\partial t}\pm q_s \quad (2)$$

$$\frac{\partial^2 h}{\partial x^2}+\frac{\partial^2 h}{\partial y^2}+\frac{\partial^2 h}{\partial z^2}=0 \quad (3)$$

In the present study, the finite difference method was employed within the MODFLOW numerical code to solve the differential equations and perform three-dimensional groundwater flow simulation under both steady-state and transient conditions.

2.3. Conceptual model development

The development of a conceptual model represents the most fundamental and critical stage in groundwater flow modeling. The relevant data and information required for modeling groundwater flow are typically categorized into hydrological and physical datasets (Anderson and Woessner, 1995). The purpose of constructing a conceptual model is to simplify the actual conditions of the study area. This involves integrating hydrological data (such as aquifer water table levels, hydraulic conductivity values and their spatial distribution, abstraction rates from pumping wells, recharge rates from precipitation and surface water flow) together with physical data (including the boundaries of the target aquifer, the location of existing rivers, information on bedrock elevations, geological and topographical maps, aquifer input and output boundaries, and drilling logs of production and observation wells), as well as supplementary information.

A pumping well refers to a well that is used for groundwater extraction for domestic, agricultural, or industrial purposes. The depth of the bedrock in the Kerman Plain, based on drilling reports of exploratory wells (1961) obtained from the Kerman Regional Water Company. Based on the data coverage, the uncertainty in depth is estimated to range from ±5 meters, depending on the location. For modeling the Kerman Plain, the required information included drilling logs of production and observation wells, precipitation and evapotranspiration data, abstraction rates from pumping wells, groundwater levels of observation wells or existing piezometers across the plain, as well as transmissivity and the thickness of alluvial deposits.

These data were obtained through the Kerman Regional Water Company and the Water Resources Studies Office of Kerman Province. The definition of initial and boundary conditions is essential for solving partial differential equations in groundwater modeling. These conditions enable the model to initiate calculations using primary and actual values prescribed by the modeler, thereby generating and evolving the hydraulic head throughout the simulation. Both spatial and temporal specifications of these conditions are required in the modeling process. The initial and boundary conditions involve the assignment of hydraulic head values to each active cell, as well as to cells with fixed hydraulic head (constant head cells) within the model (Chitsazan and Keshkooli, 2002).

For the development of the conceptual model, nine data layers were utilized, comprising water level measurements from 27 observation wells, information from 846 pumping wells, hydrogeological characteristics of the aquifer, and details regarding boundary conditions, bedrock, and regional topography. Boundaries identified as permeable on the geological map, through which flow occurs, are considered the inflow and outflow boundaries of groundwater. The inflow and outflow boundaries for the aquifer were thus defined as either permeable or impermeable based on the regional geological map. Following discretization of the study area using the PCG2 package, a uniform grid with a cell size of 300×300 m was generated, consisting of 103 rows and 134 columns. This grid size was selected due to the large area of the aquifer and to minimize computational time. The compiled datasets were organized as separate information layers using various software platforms such as GIS.

These generated layers were then assigned to the corresponding cells, so that governing equations and mathematical relationships for each cell could be computed accordingly. Upon verifying the accuracy of the simulated model, the model was executed and the unknown values were calculated. After inputting the initial data and constructing the conceptual model, the model was run under steady-state conditions in two stages. The geographic location and distribution of observation and pumping wells, as well as the map of groundwater inflow and outflow boundaries for the aquifer, are shown in Figure 2. Owing to their favorable spatial distribution within different parts of the aquifer (Bedagh-Abad (north), Esmail-Abad (south), Bolboluyeh (east), and Chari Lands (west)) and the consistency of their observed groundwater-level fluctuations with the prevailing conditions of the surrounding areas, these wells were selected as representatives of the respective sectors of the aquifer in the present study.

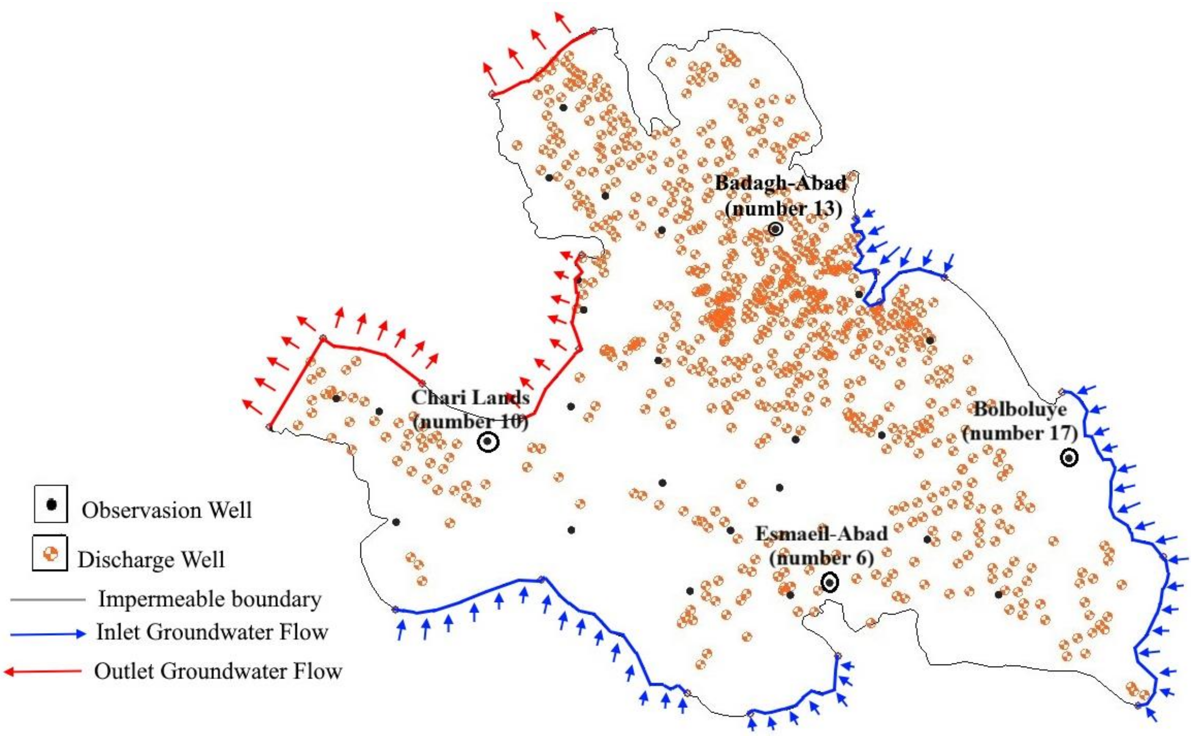

Fig. 2. Map of the geographic locations of the observation wells (four wells located in the north: Bedagh-Abad well; south: Esmail-Abad well; east: Bolboluyeh well; and west: Chari Lands well) and the pumping wells, along with the groundwater inflow and outflow boundaries of the aquifer

2.4. Steady and unsteady state modeling

Following the development of the conceptual model, steady state modeling was first performed using the initially defined values. In the subsequent stage, calibration of parameters such as anisotropy, hydraulic conductivity, and recharge from precipitation was carried out. The calibration process continued until the best results were obtained, minimizing the error between the computed and observed groundwater levels.

The unsteady state (third stage) was implemented after interpolating the specific yield parameter and importing the optimized values of anisotropy, hydraulic conductivity, and recharge from the second stage (The final time step of calibration in the steady state period). Thereafter, a second round of calibration for these parameters was conducted in the fourth stage, corresponding to the defined time steps.

2.4.1. Anisotropy

Anisotropy refers to a property of a material (such as rock, soil, or an aquifer) in which its physical or hydraulic characteristics differ depending on direction. In hydrogeology and soil mechanics, anisotropy is often defined in terms of the ratio of hydraulic conductivity in different directions (Equation 4). If this ratio equals 1, the material is considered isotropic; if it is greater or less than 1, the material is anisotropic (Alizade, 2008).

$$Anisotropy = \frac{K_x}{K_y} \qquad (4)$$

An exact initial value for horizontal hydraulic conductivity anisotropy (HANI) was not provided in the field and laboratory measurement reports from Kerman water resources studies. Therefore, in the absence of this parameter, an initial value of one was assigned to all cells. In the second stage, these values were entered into the model as pilot points using kriging interpolation, and the corresponding optimized values were then calculated.

2.4.2. Hydraulic Conductivity

Hydraulic conductivity (HK) is one of the most important physical properties of porous materials (such as soil or rock), reflecting their capacity to transmit water as a result of differences in hydraulic head or water pressure. In other words, hydraulic conductivity indicates the rate at which water can move through a saturated medium. The higher the hydraulic conductivity of a material, the more easily and rapidly water can flow through it.

To calculate hydraulic conductivity, transmissivity values were extracted from transmissivity contour lines interpolated in GIS software, while the thickness values of the Kerman Plain alluvium were obtained from the Kerman water resources study reports. Subsequently, using Equation (5), the computed hydraulic conductivity values were introduced to the model as pilot points in the GMS software and, through kriging interpolation, the parameter values for the entire aquifer were estimated. The computations for hydraulic conductivity at each pilot point are presented as an example in Table 1 (Alizade, 2008).

$$\mathrm{T} = \mathrm{K.b} \qquad (5)$$

b represents the aquifer thickness at different locations (m), T is the transmissivity coefficient $\left(\frac{m^2}{s}\right)$, and K denotes the hydraulic conductivity coefficient $\left(\frac{m}{s}\right)$ (Hydrology reports of Kerman Regional Water Company, 2020).

Table 1. The process of calculating the hydraulic conductivity coefficient at different points in aquifer

Row	Longitude (UTM)	Latitude (UTM)	Place name	$b(m)$	$T\ (\frac{m^2}{day})$	$k\ (\frac{m}{day})$
1	473934	3342423	Sadi	123.6	700	5.6
2	494264	3335403	Baghin plain	102	750	7.34
3	493161	3356907	Nozari	101.2	550	5.4
4	516346	3346568	Mahan road	102.53	800	7.8

2.4.3. Specific Yield and Storage Coefficient

Specific yield refers to the volume of water released from a unit area of an unconfined aquifer due to a unit decline in the water table. The storage coefficient denotes the volume of water expelled or absorbed per unit surface area of the aquifer as the potentiometric surface falls or rises by one unit, relevant to confined aquifers. The Kerman Plain aquifer is classified as unconfined. The value of specific yield used in the third stage of modeling (unsteady period), based on field and laboratory measurements reported in the drilling logs of observation and exploratory wells in the Kerman Plain, was set at 5% for all cells of the aquifer (Kerman Regional Water Company Reports, 2021). In the fourth stage (unsteady calibration period), these values were entered into the model as pilot points and further calibrated to achieve optimal values.

2.4.4. Aquifer Recharge

Recharge from precipitation and flood discharge in the Kerman Plain aquifer was calculated based on the long-term evaporation rate for the study area, reported as 2,530 mm per year, and the approximate 25-year average recharge discharge for the aquifer, estimated at 87.7 cubic meters per second. The infiltration resulting from precipitation was calculated monthly for the existing meteorological and hydrometric stations in the region using the FAO Equation (6), as provided by the Food and Agriculture Organization in Publication No. 19.

Additionally, the 25-year average infiltration discharge to the aquifer was divided by the aquifer area and estimated monthly. The total recharge from precipitation and flood discharge was spatially interpolated across the aquifer using the Thiessen polygon method, and the results were generalized to the entire aquifer. Table (2) presents, as an example, the calculation process of total recharge from precipitation and 25-year discharge for one month (a single time step) at the Kerman Airport station

$$F = 0.8(P - C * logE)^{0.5} \quad (6)$$

E: represents the monthly potential evapotranspiration (mm), C is a constant referred to as the infiltration index or thermal infiltration index, which depends on temperature. This coefficient ranges between 0 and 1 ([0 < C < 1]), and in this study, a value of C = 0.5 was adopted, P denotes the monthly precipitation (mm), F is the monthly infiltration (mm) (Hydrology reports of Kerman Regional Water Company, 2020).

Table 2. the process for calculating total Recharge from rainfall and 25-year flood flow rate for a time step

	Rain (mm/month)	long-term evapotranspiration (mm/year)	long-term evapotranspiration (mm/month)	FAO Equation (mm/month)	Recharge Rain (m/ day)
Recharge Rain	10.6	2530	210.83	2.36	0.000065
	Flood rate (Q) (m^3/s)	Flood rate (Q) (m^3/day)	Area of Aquifer (A) (m^2)	Approximate Recharge rate of earth (m^3/day)	(Q/A) (m/day)
Recharge of 25-year flood flow rate	87.7	7577280	1617910000	227318.4	0.00014
Sum Recharge					0.000205

2.5. Model Calibration

Calibration is one of the most critical steps in the modeling process. In some cases, this stage can be very time-consuming, often requiring adjustments to boundary conditions or certain parameters. During calibration, model parameters are systematically altered from their initial values to reproduce observed field conditions. In essence, calibration refers to the process of comparing model results with real world (field) data. The parameters subject to adjustment during calibration include hydraulic conductivity, recharge rate, hydraulic head, and water levels measured in observation wells. Both steady-state and transient calibration were performed using a combination of the automated PEST (Parameter ESTimation) method and the traditional trial-and-error approach. PEST is a calibration software designed for parameter estimation (Doherty, 2020).

During the calibration process using PEST, the defined parameters were refined to achieve the best possible match with observed data. During simulation, the hydraulic head at a given node (corresponding to an observation well) is compared with the calculated hydraulic head, and the relevant parameter values are adjusted until the simulated or computed value closely matches the observed hydraulic head and water level.

There are various criteria for evaluating the obtained results. Among them, the formulas for calculating the mean error, mean absolute error, and root mean square error are provided below (Anderson and Woessner, 1995). These criteria are used to analyze the residual errors. The accuracy of the model calibration stage was assessed using these statistical parameters (Equations 7–9):

$$ME = \frac{\sum_{i=1}^{n}(Predicted_i - Actual_i)}{n} \quad (7)$$

$$MAE = \frac{\sum_{i=1}^{n}|(Predicted_i - Actual_i)|}{n} \quad (8)$$

$$RMSE = \sqrt{\frac{\sum_{i=1}^{n}(Predicted_i - Actual_i)^2}{n}} \quad (9)$$

For comparing the differences between computed and observed values during calibration considering the acceptable error threshold it is essential to import observation points (piezometric wells) with appropriate spatial distribution into the model. After entering these control points and running the model, colored bars appear at these locations in the GMS software to indicate the magnitude of the calibration error, with the center aligned with the observed values. If the error falls within the acceptable range, the bar is displayed in green. If the error exceeds the acceptable range but is less than 200% of the acceptable error, the bar appears yellow. If the error exceeds 200% of the acceptable threshold, the bar is shown in red. If the date of the observed data does not correspond to the modeling period in MODFLOW, the bar is colored white. The bar chart in Figure (3) is used to display the calibration index in GMS.

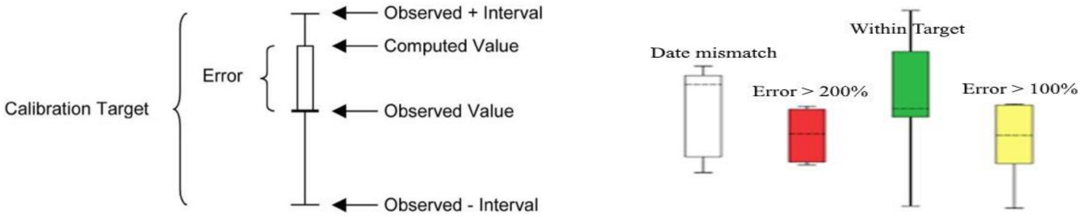

Fig. 3. Calibration index and colored bars representing observational errors at control points (modified from Connell and Bailey, 1989)

2.6. Model validation, sensitivity analysis, and prediction

Conceptually, validation is similar to calibration; however, the validation phase is performed at a different time than calibration, and while a wide range of model parameters may be adjusted during calibration, only minor adjustments are permitted during validation. For example, precipitation data can be updated, but parameters such as hydraulic conductivity or boundary conditions cannot be altered. Groundwater level prediction for the year 2024 was carried out for a period of 10 years. The results of these predictions are presented in the following sections.

2.7. Aquifer recharge through natural drainage of wastewater and effluent in Kerman city

The process of transferring urban wastewater whether naturally or artificially to groundwater aquifers is referred to as aquifer recharge. In arid and semi-arid regions, this method, especially when accompanied by additional soil filtration, can help control and prevent land subsidence, reduce evaporation and water losses, decrease the high costs associated with advanced wastewater treatment, and serve as an effective strategy for addressing water scarcity challenges (Eslamian et al., 2009).

Treated effluent, as a water resource, offers two main advantages: 1. it is largely unaffected by drought conditions, making it a reliable source. 2. it can be considered a suitable alternative to water resources that would otherwise require expensive extraction via dam construction or water transfer projects, often causing significant environmental damage. Today, the use of these recycled resources and their allocation for aquifer recharge is considered essential in modern water management (Hassanpour and Khazimenajad, 2018).

From the early development of Kerman City until 2018, municipal wastewater naturally recharged the lower aquifer of the region through absorption wells. Guided by the natural land slope, this drainage proceeded toward aquifer discharge points and the wastewater treatment plant in the northern part of the city. Over the years, this process of natural urban wastewater drainage has not only contributed to groundwater recharge but has also mitigated the risks of water source contamination. The combined recharge from precipitation, long-term flood discharge (Table 2), and natural wastewater drainage up to 2018 significantly reduced both the gradient and rate of groundwater level decline, contributing to the delayed lowering of the water table to the bedrock in the study area. Since 2018, approximately 24,138,000 cubic meters of urban wastewater per year have been redirected to a sewer network and transferred via pipelines for industrial use in neighboring basins.

Unfortunately, this diversion and the consequent cessation of natural drainage have led to an increase in the groundwater level decline rate and gradient within the Kerman urban area and the northern part of the aquifer. The results of model simulations and the evaluation of the impact of wastewater transfer as well as predictions regarding continued or discontinued transfer on groundwater level decline are presented in the following sections.

3. Results and Discussion

3.1. Steady and unsteady state modeling

Simulation of Groundwater Levels under steady and unsteady State Conditions Simulation of groundwater levels in the steady state condition is time-independent and is carried out using constant boundary and initial conditions. In contrast, for the unsteady state, groundwater level simulation is time-dependent and incorporates time-varying boundary and initial conditions. For this study, the steady state period was defined as the average water level over the first three months of 2002. The transient modeling period extends from the fourth month of 2002 to 2019, using 80% of the available data in 210-time steps.

Model validation was performed for the period from 2019 to 2024, utilizing 20% of the available data in 60-time steps. The reason for selecting the 2002–2024 period for this modeling is the availability of observational data for the study area and their more complete and accurate recording during this period by the Kerman Regional Water Company.

In addition, this period of more than two decades is widely accepted in many hydrological studies and effectively reflects both climatic and human impacts in various modeling approaches. According to the results, acceptable values of the Root Mean Square Error (RMSE), Mean Absolute Error (MAE), and Mean Error (ME) after calibration for all three periods steady state, Unsteady, and validation are presented in Table 3.

Table 3. Result of Root Mean Square Error, Mean Absolute Error and Mean Error in 3 periods

periods	RMSE	MAE	ME
Steady period	0.3	0.06	0.048
Unsteady period	0.59	0.21	-0.01
Validation period	0.06	0.54	0.61

Figure 4 illustrates the spatial distribution of observation wells and the groundwater level zoning map at the final time step for both the steady-state and transient periods. According to the groundwater level zoning for the steady-state period (Figure 4 (a)), the highest water table elevations are identified in the southeastern part of the aquifer, while the lowest levels occur in the northern and northwestern regions. In the transient period map (Figure 4 (b)), the number of observation wells is lower than in the steady-state period due to some wells having dried up or groundwater levels not being measured.

The results of the best fit between model outputs and observed groundwater level data in the fourth stage, namely the calibration phase during the transient period, are presented as time series plots of groundwater levels in four representative wells located in the north (Bedagh-Abad well), south (Esmail-Abad well), east (Bolboluyeh well), and west (Chari Lands well) of the aquifer.

Figure (5) includes four time series plots, where the horizontal axis represents the date (210-time steps) and the vertical axis displays groundwater level (in meters).

These plots illustrate the changes and decline in groundwater levels during the calibration period (2002–2019). The results indicate that after calibration, the model has successfully simulated the groundwater level fluctuations, and the deviation between the simulated and observed data remains within an acceptable range. In the plots, green data points and error bars denote the measured values and the associated uncertainty range. The error bars represent the uncertainty of either the measured or simulated data and highlight the importance of using accurate data and proper model evaluation. The overall trend in all four wells demonstrates a gradual decline in groundwater levels throughout the study period, mainly due to intensive groundwater withdrawal and reduced aquifer recharge.

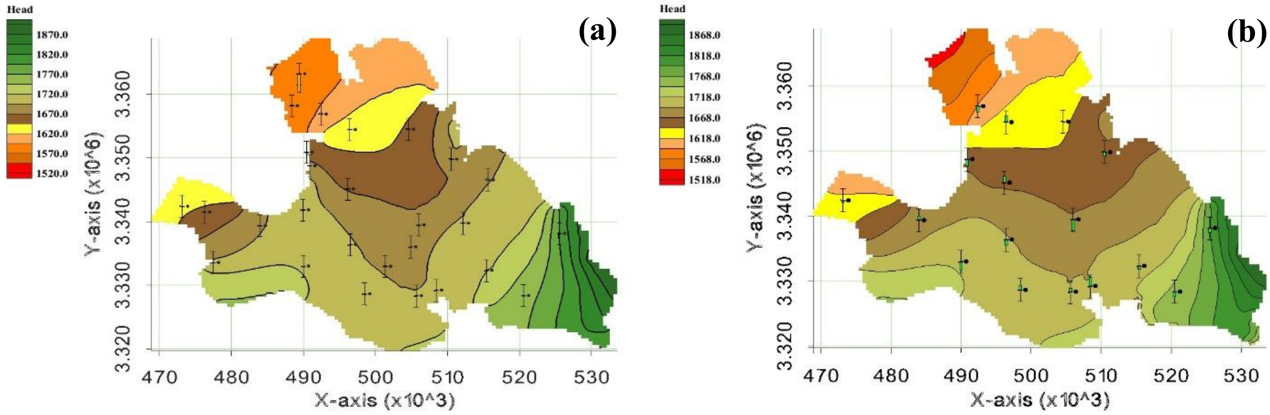

Fig. 4. (a) Groundwater level map of the Kerman Plain aquifer at the final time step of the steady period; (b) Groundwater level map at the final time step of the unsteady period

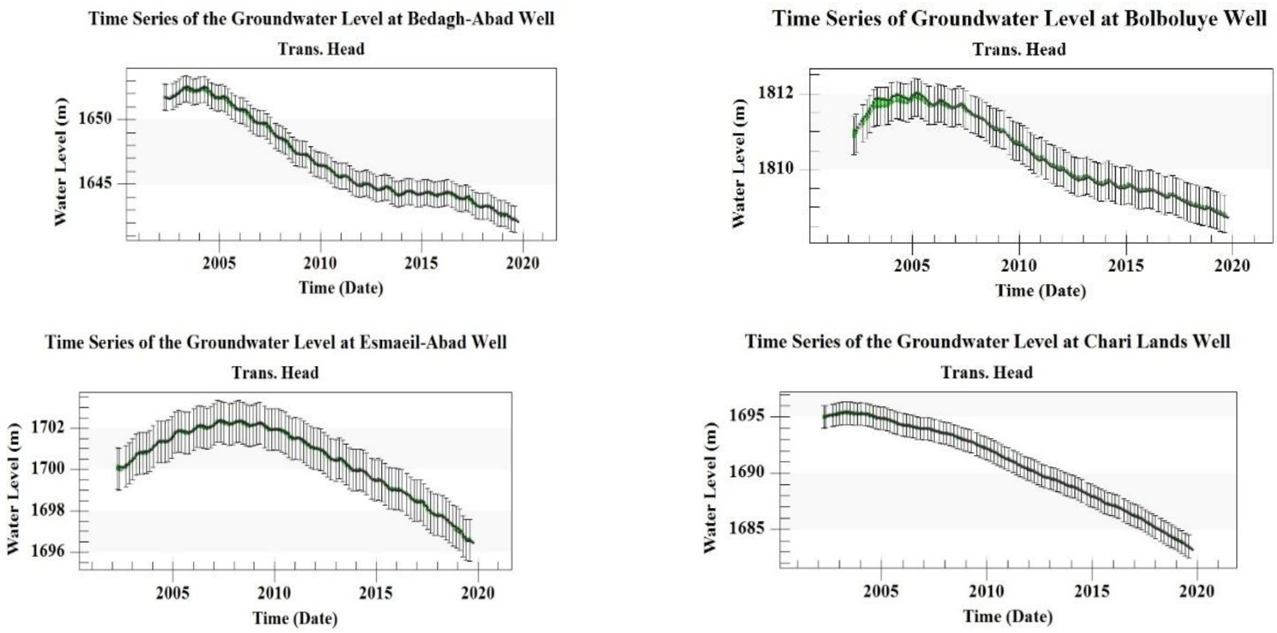

Fig. 5. Time series plots of simulated groundwater levels at four representative wells in different zones of the aquifer during the calibration period

Figure 6 presents the comparison plot of computed (Y-axis) versus observed groundwater levels (X-axis) for 27 observation wells in the study area during the fourth modeling stage. Each marker in the plot represents the data from one well at a specific time step. The tight clustering of data points around the 45-degree (equivalence) line indicates the high accuracy and strong agreement between the model results and field measurements. The coefficient of determination (R^2) was calculated as 0.99, confirming the excellent linear relationship and high model precision in simulating groundwater levels. These results are of significant importance for sustainable management and optimal exploitation planning of the region's groundwater resources, demonstrating the reliability of the model for further analyses, such as scenario development and future aquifer status prediction.

The zoning maps of the optimized parameters of Anisotropy (HANI), Hydraulic Conductivity (HK), and Specific Yield (SY) from the fourth modeling stage (calibration phase) during the transient period are presented in Figure (7 (a, b and c)). The anisotropy coefficient ranges from 0.59 to 2.8 in the provided map. The calibrated hydraulic conductivity values vary between a minimum of 2.02 and a maximum of 44.92 m/day. The northern, western, and a limited eastern part of the aquifer, due to coarse-textured sediments and high permeability, exhibit high hydraulic conductivity values (ranging from 12.44 to 30 m/day). In contrast, the central, southern, and southeastern areas, characterized by fine-grained deposits and low permeability, show minimal hydraulic conductivity values (ranging from 2.11 to 10 m/day). The calibrated specific yield (SY) in Figure (7 (a)) varies from 0.01 to 0.299, with the highest values in the western and northwestern zones and the lowest values in the eastern, southeastern, and a small part of the western aquifer area.

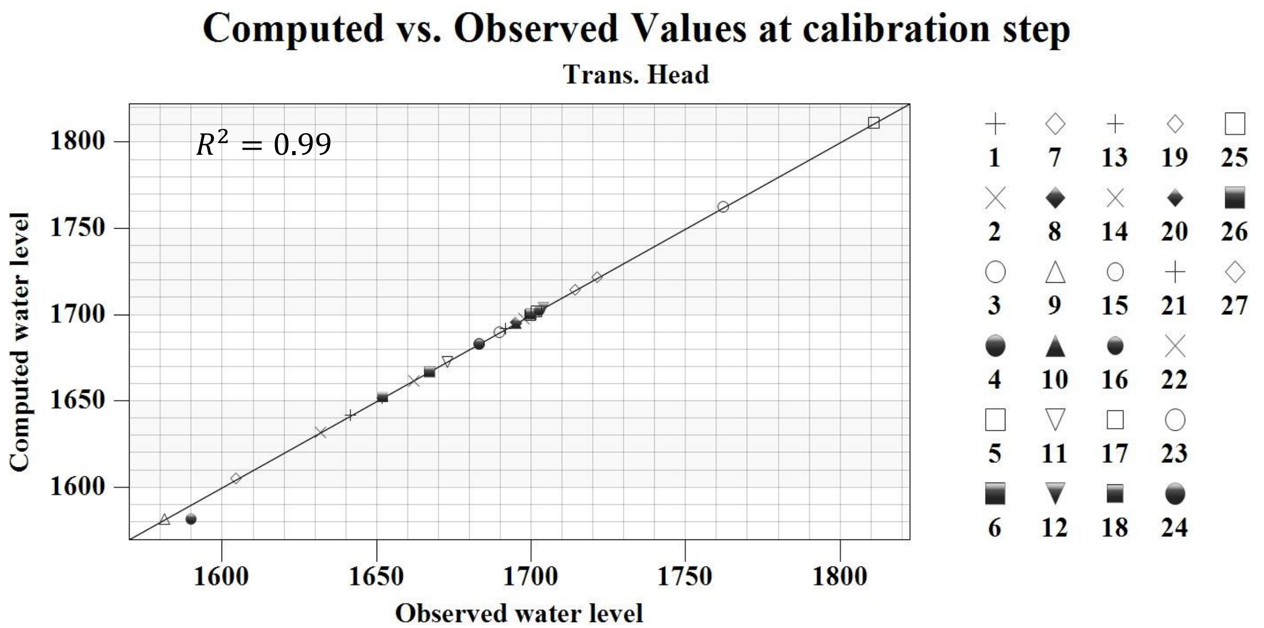

Fig. 6. Comparison plot of measured and computed water levels during the calibration period

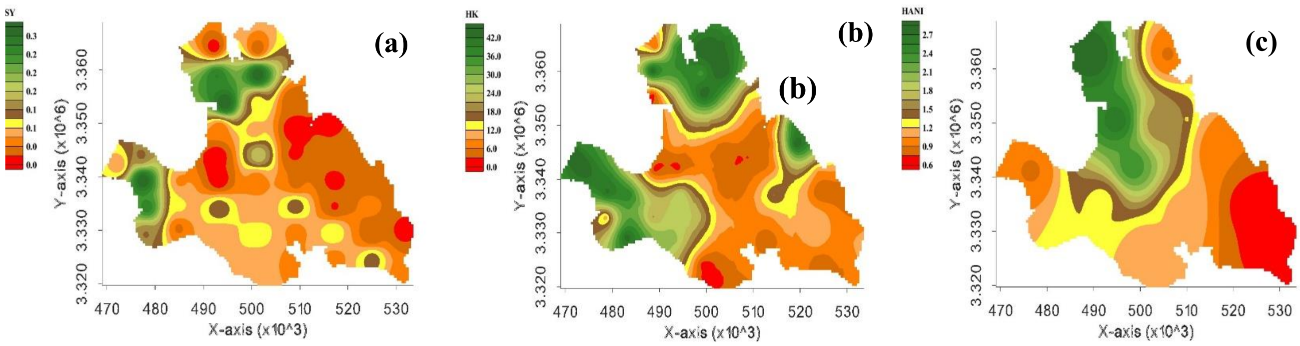

Fig. 7. Zoning maps of Specific Yield (a), Hydraulic Conductivity (b), and Anisotropy coefficients (c) of the Kerman plain aquifer, obtained from model results during the unsteady period

3.2. Validation

The suitable spatial distribution of the 17 observation wells during the validation stage, together with their coverage of diverse hydrogeological conditions and the completeness of historical groundwater level measurement records, has led to their selection and retention until the end of this stage. This selection ensured that the validation process could encompass both local and regional variations in groundwater behavior. The time series of groundwater level fluctuations for four sample wells during the fifth modeling stage (validation period) (2019–2024) in four different zones of the aquifer is presented in Figure (8).

Similar to the calibration period, the horizontal axis shows the date (60-time steps), and the vertical axis represents groundwater level (in meters). As observed, after calibration, the model has successfully reproduced the gradual decline in groundwater level during the validation period. The good agreement between model results and observed data during this period indicates the reliability and accuracy of the model in predicting future groundwater table trends in the regional aquifer. Furthermore, Figure (9) with a coefficient of determination (R^2) of 0.96 confirms the acceptable correlation and agreement between the computed groundwater levels (Y-axis) and the measured values (X-axis) for 17 observation wells during the validation period.

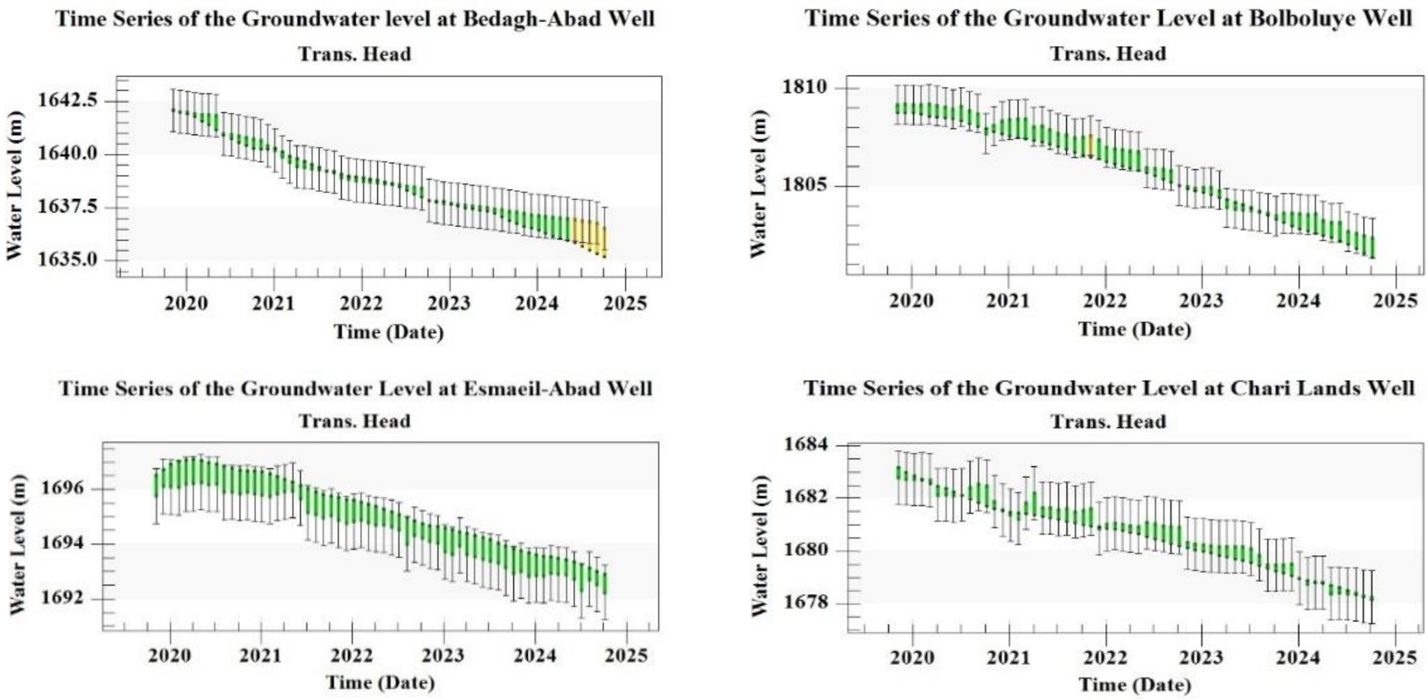

Fig. 8. Time series plots of simulated groundwater levels at four representative wells in different zones of the aquifer during the validation period

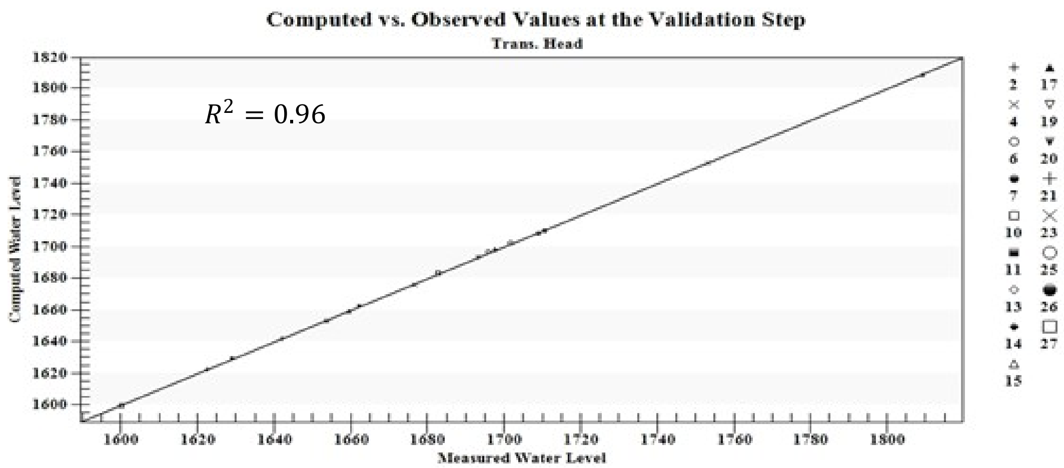

Fig. 9. Comparison plot of measured and computed water levels during the validation period

3.3. Sensitivity analysis

The results of the sensitivity analysis for the parameters estimated during the model calibration stage are illustrated in the plot shown in Figure (10). Due to the length of the chart, it has been divided into two parts and presented side by side in Figure (10 (a and b)). The key parameters at this stage include hydraulic conductivity (HK) and specific yield (SY), with the sensitivity of each parameter assessed in relation to the model target (groundwater level). The horizontal axis represents the parameter names (each corresponding to a specific location or pilot point within the aquifer), while the vertical axis indicates the sensitivity value for each parameter. As illustrated in the chart, the highest sensitivity values correspond to the HK (hydraulic conductivity) parameters at pilot points 13 (center of the aquifer), 40, and 45 (southern part of the aquifer).

These values indicate that variations in hydraulic conductivity at these locations have the greatest impact on the model simulation accuracy. Any error or inaccuracy in these areas could result in significant disruption of the model outputs. These points often coincide with zones of higher well density, lithological variability, or major hydraulic flow pathways. In contrast, the highest sensitivity values for the SY (specific yield) parameters at points 1 (north of the aquifer) and 32 (south of the aquifer) are much lower, indicating that specific yield has a considerably smaller influence on output variability compared to HK.

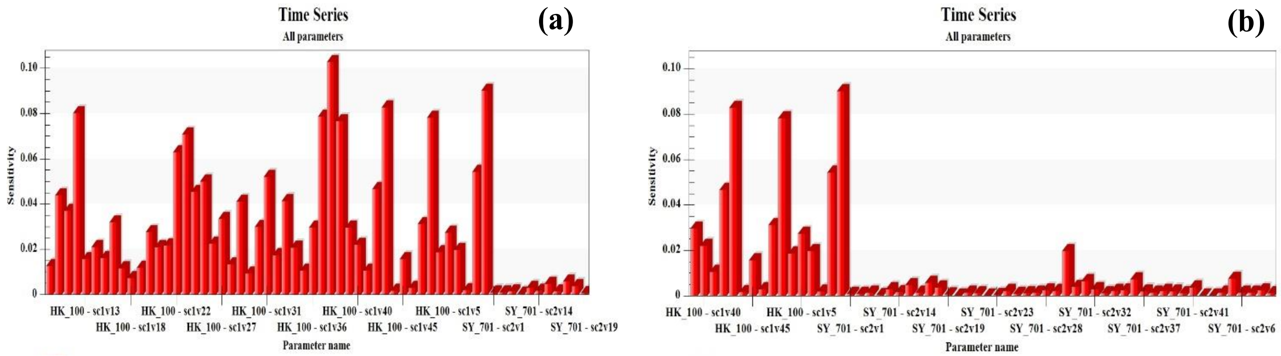

Fig. 10. Sensitivity analysis plot of the calibrated parameters during the calibration stage

3.4. Determination of groundwater level decline during the modeling and forecasting period

Following the 22-year groundwater level modeling, the future status of the aquifer was projected for a 10-year period (from October 2024 to October 2034). Figure 11 presents the modeled groundwater level decline curves from the beginning of the stable period to the end of the validation period and the subsequent 10-year forecast period.

According to these graphs, the maximum annual decline in the western and eastern parts of the aquifer averaged 1.23 meters per year, while the minimum decline occurred in the central and southern parts, averaging 0.27 meters per year.

Factors such as urban growth and population concentration in the eastern and western parts of the aquifer (due to the expansion of Kerman city in these areas), along with a significant reduction in recharge from precipitation and, conversely, an increase in groundwater extraction to meet domestic and agricultural demands, have been identified in recent years as key contributors to the increased rate of water table decline in these sections. These factors, despite the favorable influence of coarse-grained soil texture and high permeability in the western regions and in a limited area of the eastern aquifer, have resulted in a water table decline rate of 1.23 m/year.

In contrast, over the past 22 years, the slower pace of villa construction and lower population density in the central and southern parts of the aquifer compared to the eastern and western parts combined with the lowest hydraulic conductivity values, limited distribution of pumping wells, and restricted groundwater extraction in these areas, have resulted in a water table decline rate of only 0.27 m/year. For the purpose of forecasting and assessing the future status of the aquifer, stable conditions of recharge and discharge from the region's abstraction wells were assumed, remaining unchanged and consistent with the last time step of the validation period.

The results of the 10-year forecast period indicated that the maximum groundwater level decline in the eastern and southeastern parts of the study area will average 2 meters per year, while the minimum annual decline 0.78 meters will occur in the central, northeastern, and southern parts of the aquifer. The spatial distribution of groundwater level decline in the Kerman Plain during the modeling and forecasting periods, used to better illustrate and compare the past and future states of the aquifer, is presented in Figure 12.

3.5. Prediction and comparison of the extent of groundwater level decline under scenarios with and without municipal wastewater-induced recharge

The use of wastewater and treated effluent for aquifer recharge through natural drainage via absorption wells has been recognized as a low-cost, efficient, and highly effective management strategy for improving critical aquifer conditions. In recent years, the treated municipal wastewater of Kerman city, located in the north of this prohibited plain, has been transferred to an adjacent basin for industrial use.

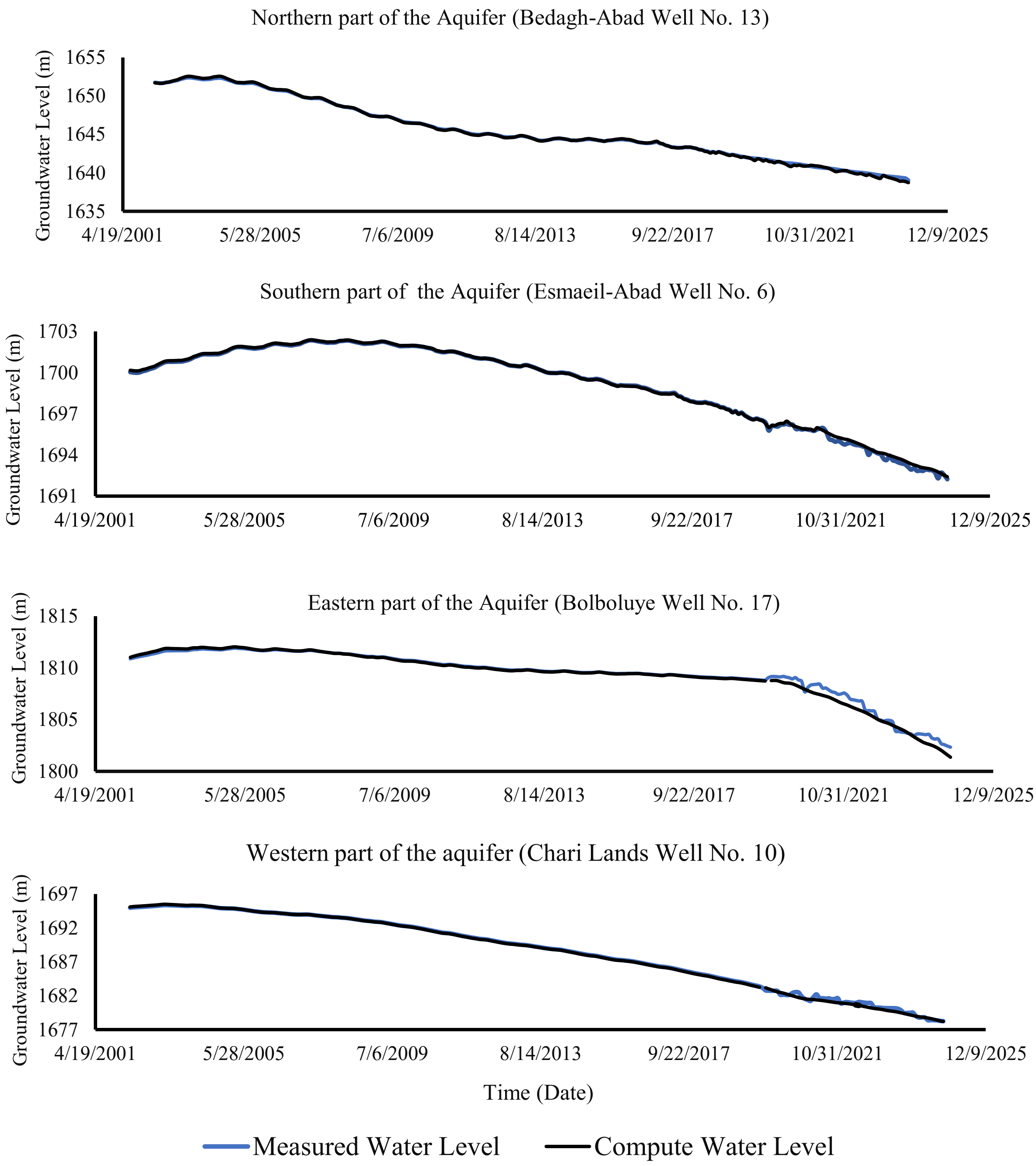

Fig. 11. Chart of Observation and Modeling Groundwater Level 4 wells in the North, South, East and West of Aquifer

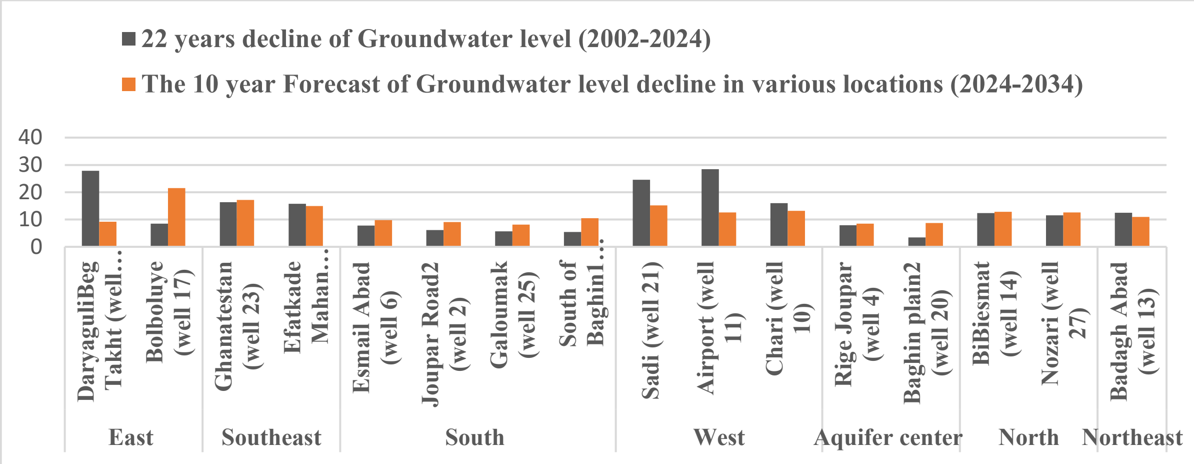

Fig. 12. Modeled and forecasted groundwater level decline in the Kerman Plain aquifer

Prior to its transfer to the adjacent basin, this wastewater contributed to the natural recharge of the aquifer within the urban area and to artificial recharge in certain northern parts of the aquifer (the Ekhtiar-Abad and Zangi-Abad region), thereby reducing the rate of groundwater level decline in the area.

In the following sections, the modeling and prediction of the effects of natural drainage and the absence of recharge from treated wastewater on the groundwater level decline in the plain are discussed. For this purpose, the groundwater level of the Bedagh-Abad observation well, located in Kerman County, was simulated under two scenarios: first, under current conditions without the influence of wastewater, and second, considering the effect of wastewater from 2018 (the year when wastewater transfer for industrial use began) until 2024. Forecasting was then carried out from 2024 onward until the groundwater level reached the average bedrock elevation within the urban area of Kerman. According to the results of the 7-year (2018–2024) modeling, in the first scenario, the groundwater level declined at an estimated rate of 62.60 centimeters per year.

Furthermore, if the transfer of wastewater for industrial purposes continues and no recharge occurs through drainage into the aquifer (current conditions), the groundwater in the city of Kerman will reach the bedrock by the year 2044. Modeling and forecasting were again conducted under the second scenario, in which the continuation of natural wastewater drainage through absorption wells represented as an increase in the volume of recharge from wastewater and treated effluent (m/day) was added to the recharge from precipitation within the urban polygon of Kerman. The results indicated that, with natural wastewater drainage during the same 7-year modeling period (2018–2024), the rate of groundwater level decline was reduced by 15.85%, and was calculated to be 51 centimeters per year.

Furthermore, with the continuation of natural wastewater drainage, the year in which the groundwater reaches the bedrock in this city is projected to be 2058. Therefore, it can be concluded that the difference in the timing at which the groundwater level in the two scenarios reaches the average bedrock elevation of the study area indicates the effect of the presence or absence of recharge resulting from natural drainage. The validity and interpretation of the 15.85% increase in the rate of decline due to wastewater diversion were confirmed by comparing this value with the increase reported in a similar study. Mirkamandar et al. (2025), instead of scenario modeling, predicted the historical trend of the natural slope of groundwater level decline under conditions with and without recharge from wastewater in the Nozari well.

Their results, despite the distance between the studied well and the city of Kerman, indicated an 11% increase in the rate of decline caused by wastewater diversion. This finding corroborates the 15.85% increase in the rate of decline due to wastewater diversion for the studied Bedagh-Abad, which is located near the city center of Kerman. The observed difference of 4.85% between the two studies is attributed to the distance between the wells. Our studied well, being geographically closer to the city center, is subject to greater recharge compared to the Nozari well investigated in the aforementioned research.

The graphs presented in Figure 13 illustrate the measured groundwater level in the Bedagh-Abad observation well within the urban area of Kerman, the modeled and forecasted groundwater levels under both recharge and no recharge conditions (resulting from natural or artificial drainage), as well as the average bedrock elevation of Kerman city. According to these graphs, the average bedrock elevation within the urban area is 1624 meters.

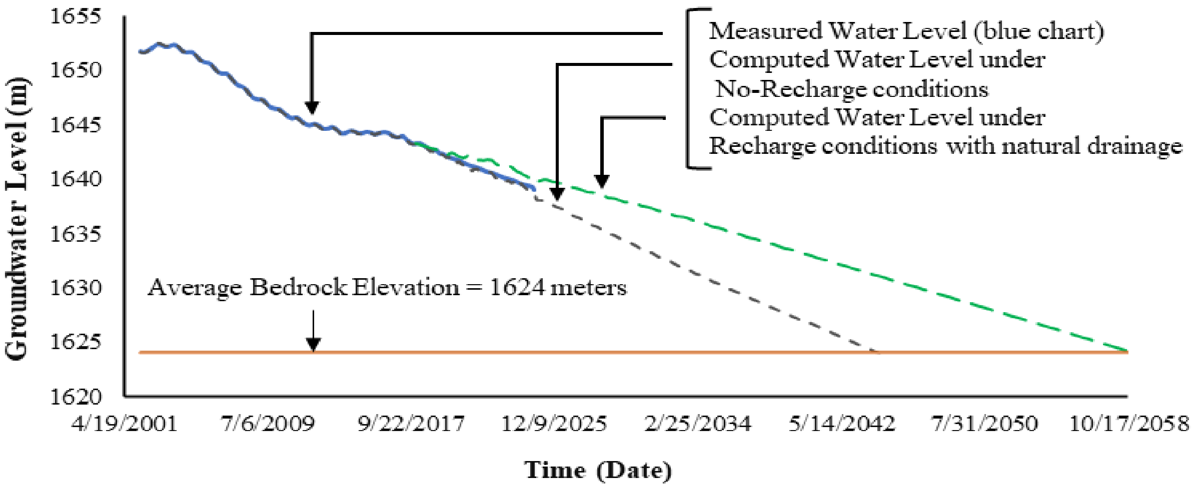

Fig. 13. Forecast and Comparison of Groundwater Level decline under conditions with and without natural drainage and artificial recharge using municipal wastewater

3.6. Management scenarios

The critical condition of the aquifer necessitated the implementation of various management scenarios to forecast the 10-year groundwater level trends in the plain and to provide appropriate management strategies. The above results revealed the extent to which recharge from both natural and artificial wastewater drainage could prevent groundwater level decline within the Kerman urban area.

Therefore, in addition to maintaining the current trend and enhancing recharge from wastewater, other combined scenarios were also defined, including: reduction of abstraction from pumping wells and increased recharge from precipitation. Accordingly, twelve different scenarios were introduced into the model, comprising: 10%, 20%, and 30% reduction in abstraction from pumping wells, 10% reduction in abstraction combined with 10%, 20%, and 30% increase in recharge, 20% reduction in abstraction combined with 10%, 20%, and 30% increase in recharge, and 30% reduction in abstraction combined with 10%, 20%, and 30% increase in recharge. The chart in Figure 14 illustrates historical groundwater level variations (measured data as blue lines and simulated data as black lines), future projections under different scenarios, and the impact of each on the groundwater level behavior at the Bodagh-Abad well. In the base chart, temporal groundwater level changes are shown for the period 2002–2034, covering past, future, and forecasted scenario states.

In the enlarged inset graph, the modeled projections for each defined scenario are presented for better visibility and clarity. Introducing the baseline scenario into the model maintaining the current situation with ongoing abstraction from pumping wells and constant natural recharge indicated that the aquifer's decline will accelerate, posing a serious crisis over the next decade and threatening the Kerman Plain aquifer as a primary water source for various uses.

As shown in the scenario trend chart, abstraction-reduction scenarios alone can merely slow the rate of decline, but are insufficient for completely halting or reversing the critical condition. In contrast, combined scenarios of reduced abstraction with increased natural recharge particularly at the 30% level could place groundwater conditions at the target well and surrounding areas at the stability threshold, yielding the greatest improvement and control over the critical situation.

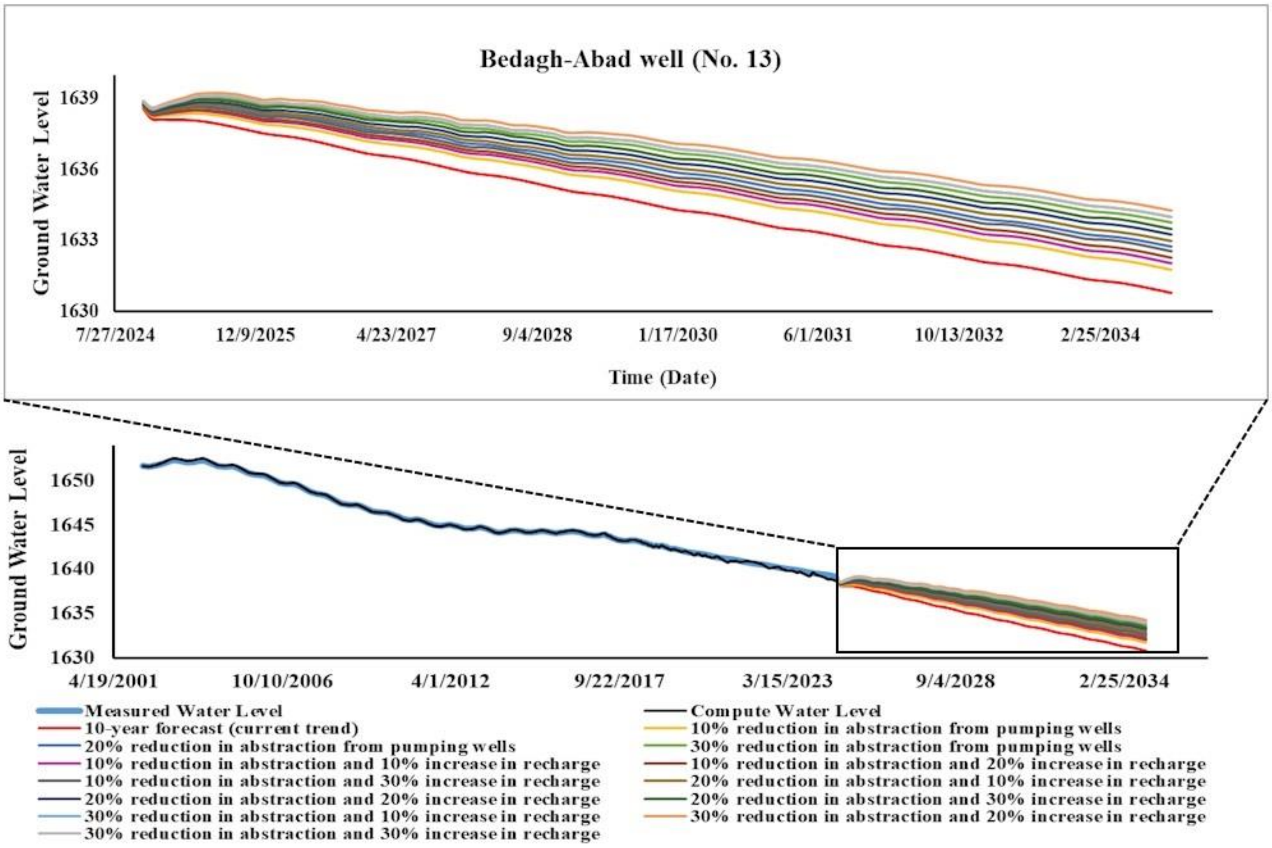

Fig. 14. The chart of Groundwater level variations at the Bedagh-Abad well under different scenarios

4. Conclusion

Modeling of the past 22 years showed that the maximum decline in the Kerman Plain aquifer occurred in the western and eastern areas, with an average annual rate of 1.23 meters. Furthermore, forecasts for the next 10 years indicate that the maximum groundwater level decline in the eastern and southeastern parts of the study area will average 2 meters per year. According to the conducted analysis, natural drainage of wastewater through absorption wells and artificial recharge using treated wastewater are factors that reduce the rate of groundwater level decline in the urban area of Kerman by 15.85% annually. Continuation of this process would delay the time at which the groundwater in Kerman reaches the bedrock of the study area by 14 years.

Unfortunately, under current conditions, the transfer of wastewater for industrial purposes has led to an increased rate of groundwater level decline in the representative well (Bedagh-Abad well) within the urban area of Kerman and the northern parts of the aquifer, resulting in an additional annual decrease of 9.6 centimeters in the measured groundwater level data. The comparison of this study's findings with those of Kamali et al. (2021), who aimed to model and assess the effects of constructing a complete municipal wastewater collection network in the Yazd–Ardakan Plain under similar climatic conditions and groundwater level declines, and Mirkamandari et al. (2025), who aimed to calculate the groundwater level decline gradient following the transfer of wastewater to an adjacent basin in the Nozari well in the Kerman Plain, highlights the impact of wastewater-derived recharge in reducing groundwater level decline.

Considering the significant decline in groundwater levels in recent years and the projected further decreases in the future, integrated management is identified as the most effective approach to stabilizing groundwater levels. For improved management and the provision of an appropriate solution, a 30% reduction in abstraction from existing pumping wells in the region, along with the identification and removal of unauthorized wells, is recommended. Such a reduction in abstraction could moderate the rate of groundwater decline by introducing a gentler downward trend. Since variations in natural recharge are influenced by climatic and hydrological factors making them difficult and beyond direct control artificial recharge methods can be considered an effective measure. In this regard, creating artificial recharge conditions through the use of raw and treated wastewater, aiming to provide approximately 30% of the required recharge and conveying it to subsurface layers, is proposed as a practical and manageable solution to improve the quantitative condition of the aquifer.

These findings may serve as an effective and appropriate management strategy to address both the current and future crises of drought and water scarcity and as a basis for decision-making by regional water policymakers in selecting the optimal management scenario. Also, although the hydrogeological characteristics of the Kerman aquifer are unique, the conceptual framework for evaluating the impacts of wastewater diversion on groundwater drawdown under various recharge and pumping scenarios can also be applied to other aquifers in arid regions with similar rainfall patterns, evaporation rates, and geological conditions.

5. Disclosure Statement

No potential conflict of interest was reported by the authors

6. References

Alizadeh, A. (2008). *Principles of applied hydrology* (20th ed.)

Anderson, M. P., Woessner W. W. (1995). APPLIED GROUNWATER MODELING. Simulation of Flow and Advective Transport (Second Edition).

Azizi, F., Asghari Moghaddam, A., & Nazemi, A. (2019). Groundwater Flow and Salinity Intrusion Simulation in Malekan Plain Aquifer. *Iranian Journal of Watershed Management Science and Engineering, 13*(45), 32-43. http://jwmsei.ir/article-1-769-fa.html.

Bahir, M., Ouhamdouch, S., & Carreira, M. (2018). Isotopic and geochemical methods for studying water–rock interaction and recharge mode: application to the Cenomanian–Turonian and Plio-Quaternary aquifers of Essaouira Basin. Morocco, *Marine and Freshwater Research*, *69*(8), 1290-300.

Bahir, M., Ouazar, D., Goumih, A., & Ouhamdouch, S. (2019). Evolution of the chemical and isotopic composition of groundwater under a semiarid climate; the case of the Cenomano-Turonian aquifer within the Essaouira basin (Morocco). *Enviromental Earth Sciences*, 78:353. https://doi.org/10.1007/s12665-019-8349-2.

Baki, S., Hilali, M., Kacimi, I., Kassou, N., Nouiyti, N., & Bahassi, A. (2017). Assessment of groundwater intrinsic vulnerability to pollution in the Pre-Saharan areas-the case of the Tafilalet Plain (Southeast Morocco). *Procedia Earth and Planetary Science*, *17*, 590-593.

Bayatvarkeshi, M., Fasihi, R., & Zareabyaneh, H. (2018). Numerical simulation of groundwater flow path in Hamedan-Bahar aquifer. *Iranian Journal of Health and Environment, 11*(1), 49-62. http://ijhe.tums.ac.ir/article-1-5975-fa.html.

Bejranonda, W., Koch, M., & Koontanakulvong, S. (2009, February). Improving traditional conjunctive use management with surface water and groundwater dynamic interactions modeling. In *International Symposium on Efficient Groundwater Resources Management (IGS-TH 2009), Bangkok, Thailand*.

Carreira, P.M., Bahir, M., & Salah, O. (2018). Tracing salinization processes in coastal aquifers using an isotopic and geochemical approach: comparative studies in western Morocco and southwest Portugal. *Hydrogeol, 26*, 2595–2615. https://doi.org/10.1007/s10040-018-1815-1.

Chitsazan, M., & Kashkuli, H. (2002). Groundwater modeling and solving hydrogeological problems. Shahid Chamran University of Ahvaz, First Edition, (In Persian).

Connell, J. F., & Bailey, Z. C. (1989). *Statistical and simulation analysis of hydraulic-conductivity data for Bear Creek and Melton Valleys, Oak Ridge Reservation, Tennessee* (No. 89-4062). Department of the Interior, US Geological Survey.

Dafny, E., Burg, A., & Gvirtzman, H. (2010). Effects of Karst and geological structure on groundwater flow: The case of Yarqon-Taninim Aquifer, Israel. *Journal of Hydrology*, *389*(3-4), 260-275.

Doherty, J., (2020). PEST - Model-Independent Parameter Estimation User Manual Part I: PEST, SENSAN, and Global Optimisers. 7th Edition, Watermark Numerical Computing.

Hasanpour, M., & Khozeymehnezhad, H. (2018). Placement of nutrient wells for artificial nutrition and improvement of aquifer quality in Birjand plain using wastewater treated wastewater. *Journal of Research in Environmental Health*, 4(3), 215-226. 10.22038/jreh.2018.33951.1235.

Hosseinzade Kuhi, H., & Ardestani, M. (2022) Modeling and quantitative investigation of the groundwater condition of the South Mehyar-Dasht Asman aquifer using the MODFLOW model, *Water and Soil Management and Modeling*, *4*(1), 1-17. doi.org/10.22098/mmws.2022.11807.1172.

Islamian, S. S., Hedayat, E., & Tarkesh Esfahani, S. (2009). *Reuse of treated wastewater through groundwater recharge to sustainably increase water Resourse.* First International Conference on Water Resources with a Regional Approach, Shahrood. https://civilica.com/doc/83167 (In Persian).

Jafari Godeneh, M., Salajegheh, A., & Malekian, A. (2021). Investigating the Impact of Different Climate Change Scenarios on Groundwater Fluctuations in Arid and Semi-Arid Regions (Case Study: Kerman Plain). *Journal of Irrigation and Water Engineering*, *44*(4), 252-275. 10.22125/iwe.2021.133762 (In Persian).

Kamali, E., Bemani Kharanagh, A., Hayatzadeh, M., Sajati Ardakani, G.H., & Khalili, H. (2021). Numerical modeling of the effects of constructing an urban wastewater treatment plant on the quantity and quality of groundwater resources in Ardakan city. *Journal of Natural Environment*, *74* (1), 139-152. doi: 10.22059/jne.2021.314767.2128

Kholghi, M. (2001). Mathematical Models in Groundwater Flow: From Theory to Application. Tehran University Press, *Department of Irrigation Engineering*, Tehran, Iran, (In Persian).

Koch, M., Arlai, P., & Lukjan, A. (2012). Modeling Investigation on the future Permissible Yield in upper Chiang Rai Aquifers System. *Procedia Engineering*, *32*, 69-76. https://doi.org/10.1016/j.proeng.2012.01.1238.

Lyazidi, R., Hessane, M. A., Moutei, J. F., & Bahir, M. (2020). Developing a methodology for estimating the groundwater levels of coastal aquifers in the Gareb-Bourag plains, Morocco embedding the visual MODFLOW techniques in groundwater modeling system. *Groundwater for Sustainable Development*, *11*, 100471.

Mirkamandar, B., Rahnama, M. B., & Zounemat Kermani, M. (2025). Investigation of the Effect of Urban Wastewater Network Implementation on Groundwater Flow Dynamics (Case Study: Kerman City). *Journal of Iranian Water Engineering Researc*, IJWER-2507-1100.

Najafi, S., Sharafati, A., & Kardan moghaddam, H. (2022). Evaluating the effect of climate change on groundwater level changes in the Sari-Neka coastal aquifer. *Irrigation and Water Engineering, 13*(2), 312-332. 10.22125/iwe.2022.162660.

Nouayti, N., Nouayti, A., Khattach, D., & Hilali, M. (2020, March). Geostatistical approach for evaluating heavy metal contamination in groundwater in the high Ziz Basin (Morocco). In *Proceedings of the 4th Edition of International Conference on Geo-IT and Water Resources 2020, Geo-IT and Water Resources 2020* (pp. 1-4).

Panahi. M., Misagi, F., & Asgari, P. (2018). Simulation and estimate groundwater level fluctuations using GMS (Zanjan plain). *Advanced Environmental Sciences*, *16*(1), 1-14.

Reyhani, E., Yousefi, H., Mirzavand, M., & Sadatinejad, J. (2023). Modeling the impact of management scenarios on the Kashan aquifer with the mathematical model Modflow and Seawat. *Journal of Ecohydrology*, *10* (1), 17-32. doi: 10.22059/ije.2023.358892.1727.

Sabahnia, D., & Sadeghi Lari, A. (2024). Quantitative groundwater modeling using GMS-MODFLOW (Case study: Shamil aquifer in Hormozgan province). *Hydrogeology*, *9* (1), 71-85. https://doi:10.22034/hydro.2024.62911.131.

Sheikha BagemGhaleh, S., Babazadeh, H., Rezaei, H., & Sarai Tabrizi, M. (2023). Numerical Modeling and Trend Analysis of Mahabad Aquifer Quantitative Status. *Water and Soil Management and Modelling*, *3*(2), 1-17. https://doi.org/10.22098/mmws.2022.11275.1113 [In Persian].

Szucs, P., Szekely, F., & Zakanyi, B. (2013). Comparison of Analytical and Numerical Approaches for Simulating Groundwater Flow to Multi Screen Wells, *Carpathian Journal of Earth and Environmental Sciences*, *8*(2), 69 –76.

Taheri Tizro, A., & Kamali, M. (2019). Groundwater modeling by MODFLOW model in Toyerkan aquifer and evaluation of hydrogeological state under present and future conditions. *Water Engineering*, *12*(40), 89-104. dor: 20.1001.1.20086377.1398.12.40.8.4. [In Persian].

Yousefi, F., Jannet Rostami, S., & Mohammadi, K. (2020). Modeling the mixing zone of surface and groundwater using Modflow, MT3D and RT3D models. *Iranian soil and water research, 51* (5), 1151-1164.10.22059/ijswr.2020.285606.668264.